CERN – European Organization for Nuclear Research

European Laboratory for Particle Physics

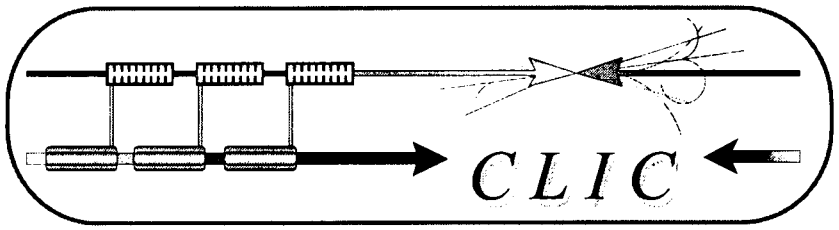

CLIC Note 429
PS/RF Note 2000-006

Simulations of beam dynamics in the CTF2 drive beam accelerator and bunch compressor.

M. CHANUDET-CAYLA

Abstract

The purpose of this study is to simulate and to have a better understanding of the experimental limitation of the transmission in the CTF2 drive beam in function of the beam charge. In this note, the low energy part of the beam line is studied with the particle-tracking program PARMELA from the gun to the first 30 GHz section. Assuming the beam loading and space charge at 10nC/bunch, the settings of the magnetic components in Nov 98 configuration are discussed and slight modification have to be proposed to obtain a good matching and total transmission until the first 30GHz section. The possible limitation of transmission in the HCS for bigger beam size generation on the cathode is pointed out. Some particularities of the bunch compressor are shown as well as the effect of the bunch correlation quality, the deflection angle limitation and the phase shift induced in the train. Finally, transverse results are resumed and the simulated total transmission is validated by experiments. Beam parameters will be used by A. Riche [5] to study the wake-fields and the beam transmission in the downstream 30GHz sections.

Geneva, Switzerland
18 April 2000

Simulations of beam dynamics in the CTF2 drive beam accelerator and bunch compressor

M. CHANUDET-CAYLA
CERN PS/RF

I. Introduction

The behaviour of the CTF2 drive beam [1] is studied from the RF electron gun to the 30GHz power extracting structures. The purpose is to create a numerical model for the beam loading in the 3GHz HCS sections and the effects of the space charge of the 10nC bunches. The beam transmission through the overall line is simulated to compare the results with CTF2 measurements on November 1998.

In this note, only the 3GHz part of the drive beam line is studied. The particle tracking program PARMELA [2] simulates the beam dynamics through the RF sections, magnetic elements and bunch compressor from the gun4 to the entrance of the first PETS (Power Extraction and Transfer Section at 30GHz).

First, the exact configuration of Nov. 98 is simulated. The inputs used in PARMELA are described and the results are quickly reported. Secondly, the settings of some magnetic elements are slightly modified to optimise the simulated beam transmission until the first PETS. The beam characteristics at the HCS sections and the first PETS are then discussed. The influence of a variation of divergence at the HCS exit is calculated. The effects of the bunch compressor are also verified as a function of its field magnitude and particle distribution.

II. Nov. 98 settings for the 3GHz part of the drive beam

In this paragraph, the 3GHz part of the drive beam line is presented in its exact Nov. 98 configuration. The main characteristics of the elements used in PARMELA are given. The emplacement and the settings of the components are recapitulated in the figure 1 and tables 1 and 2. Then, the simulations are summarised in figure 2 and table 3 and briefly discussed.

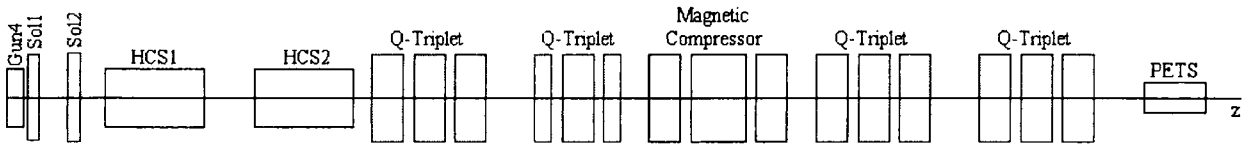

Figure 1: *Schematic layout of the CTF2 components for the Nov. 98 configuration*

		z-Position * (cm)	Length (cm)	Experimental Settings	Modified settings
Photo-cathode	†	0.0	/	∅ laser of 11mm	∅ laser of 11mm
Gun 4	†	5.6	/	100MV/m laser 30° of RF crest	100MV/m laser 30° of RF crest
Solenoid 1		17.4	5.26	3100G (90A)	3580G (105A)
Solenoid 2		47.4	7.73	1170G (50A)	1170G (50A)
HCS1 section		75.0	81.2	35MV/m -60° of RF crest	35MV/m -60° of RF crest
HCS2 section		181.5	81.5	35MV/m +25° of RF crest	35MV/m +25° of RF crest
QFN 130		270.0	22.0	84G/cm	77G/cm
QFN 131		299.8	22.0	167G/cm	167G/cm
QFN132		329.6	22.0	104G/cm	96G/cm
QFN140		524.3	12.4	54G/cm	54G/cm
QFN141		549.3	22.0	53G/cm	53G/cm
QFN142		574.3	12.4	54G/cm	54G/cm
BHZ E150		602.1	22.3	625G	625G
BHZ C151		689.1	44.6	750G	750G
BHZ E152		776.1	22.3	625G	625G
QFN160		808.7	22.0	91G/cm	77G/cm
QFN161		838.5	22.0	137G/cm	129G/cm
QFN162		868.3	22.0	81G/cm	77G/cm
QFN170		1130.2	22.0	92G/cm	106G/cm
QFN171		1160.0	22.0	163G/cm	167G/cm
QFN172		1189.8	22.0	82G/cm	95G/cm
Z=0 PARMELA		2.4		/	

Table 1: *Position and settings of the components for the exact and slightly modified Nov. 98 configuration. *The positions are given from the photo-cathode to the middle of the element except for the HCS1 and HCS2 sections where the reference is the middle of the input wave guide. † The corresponding element is not integrated in the PARMELA simulation.*

II.1 Beam representation

The train of the drive beam is constituted of 48 bunches at a repetition rate of 2998.55MHz. In the PARMELA program, each bunch is generated and simulated separately. Only the 1st , 24th and 48th bunches are calculated to sample the energies in the train with γ equal to 14., 13. and 12. respectively.

From MAFIA simulations of the gun4 by M. Dehler [3], the main characteristics of the beam are extrapolated and transposed in PARMELA simulations [4] in the case of a laser spot of about 11mm, a laser phase of 30° and a gun electric field of 100MV/m. The source of particle is then located on a virtual cathode at 100mm in front of the first solenoid and outside the magnetic field. For each bunch of 10nC, 700 macro-particles are generated. They are spread in the transverse phase space (x, x') and (y, y') according a Gaussian distribution in the phase ellipse. In the longitudinal phase space, they are generated uniformly in the ellipse (z, Energy) with a rms length of about 1mm. The table 2 resumes the input beam data used in PARMELA code.

Then, the macro particles are tracked through the different RF and magnetic components of the line with space charge assumed but no wake-field.

		Nov 98 run Virtual cathode		
bunch n°		**1**	**24**	**48**
$x_{max}=y_{max}$	**mm**	3.85	3.99	4.14
$x'_{max}=y'_{max}$	**mrad**	26.74	28.14	30.38
$\varepsilon x_{rms} = \varepsilon y_{rms}$	**mm.mrad**	48.	49.	51.
Δz_{rms}	**mm**	0.99	1.02	1.05
$\langle\gamma\rangle$		14.0	13.1	12.1
$\Delta\gamma_{rms}/\gamma$	%	1.3	1.5	1.7

Table 2: *Input beam characteristics for the PARMELA simulation of the 3GHz part of the beam line*

II.2 RF accelerating structures HCS

Along the drive beam, the bunches are accelerated until 45MeV by the two RF sections HCS1 and HCS2. A realistic model of these structures was defined and validated in the report [4]. This pattern is used in the present simulations: the two input and output couplers are represented by fully standing wave cavities. The 13 cells between the couplers are described by travelling waves operating with a phase advance of $11\pi/12$ per cell.

The average accelerating fields in the section is of about 35MV/m and the attenuation along the structure is neglected. The beam loading in the train is calculated analytically and introduced in PARMELA for each bunch by the means of lower accelerating gradients. These two structures have also their RF frequency shifted by ±7.41MHz from the bunch repetition rate of 2998.55MHz. By a judicious choice of the bunch phase in the HCS sections, the energy spread of the train induced by the beam loading is decreased and an intra-bunch correlation necessary to the following bunch compression is created. In this simulations, the first bunch arrives with a phase of -60° and +25° from the RF crest of respectively HCS1 and HCS2.

II.3 Magnetic elements and bunch compressor

In addition to the RF structures (gun and HCS), the transverse optics of the line are realised by classical magnetic elements: two solenoids immediately after the gun4 and four triplets of quadrupoles between the HCS and PETS sections. These solenoids are represented ideally in PARMELA by their effective length and their gradient extracted from their measured fields (for their individual location and characteristics see table 1).

Between the triplets, the magnetic bunch compressor is simulated in. It consists of three rectangular dipoles. Their effective length and magnetic field are chosen to generate symmetrical deflections in the horizontal x plane (also see table 1 for their values). The fringe fields of the short dipoles induce a strong quadrupolar focusing force, which is simulated perfectly by PARMELA.

II.4 PARMELA results in exact Nov. 98 configuration

According to the layout previously described, PARMELA simulations were run for the three bunches 1, 24 and 48 of the train. The variations of x and y envelopes along the z axis are presented on figure 2. The rms values of the main beam characteristics Δz, γ,$\Delta\gamma/\gamma$, x, x' and emittance for a choice of z positions are also reported in the table 3. Here, some properties of the beam dynamics along the 3GHz line are pointed out.

At the entrance of the HCS structures, the two solenoids focus the transverse envelopes of the train below a radius of 13mm, just 2mm smaller than the HCS radius aperture of 15mm. Due to the energy spread of about 1MeV at the gun exit, the different bunches arrive in HCS with a spread of radius and divergence up to ±1.5mm and ±2.3mrad respectively.

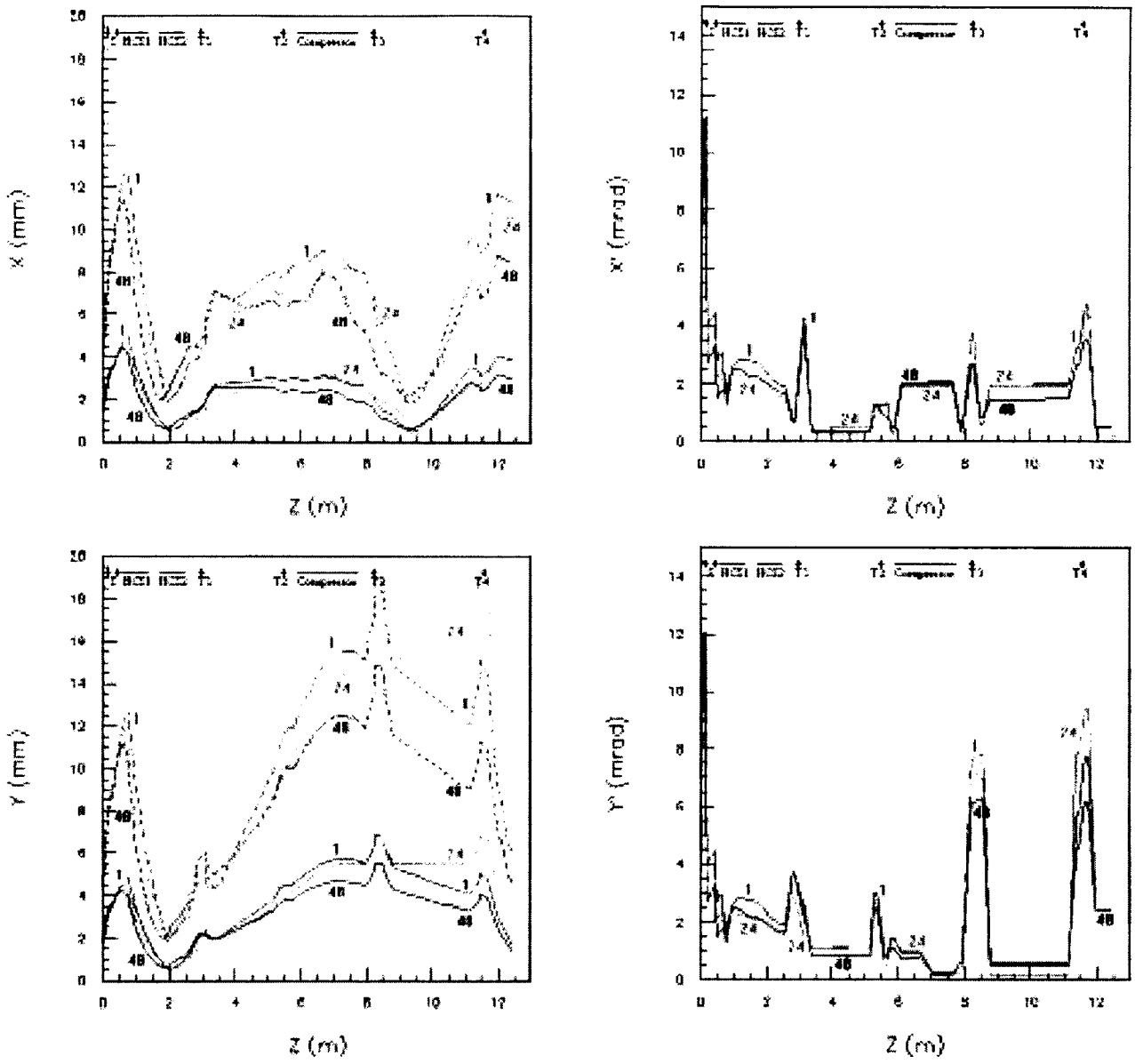

Figure 2: *x, y, x' and y' variations along the Nov 98 layout simulated with 700 macro-particles. The numbers 1, 24 and 48 (and the red, green and blue colours) refer to the 1st, 24th and 48th bunches respectively. Rms values are drawn by solid lines, maxima by dashed lines.*

As demonstrated in note [4], there is a strong focusing in the RF input coupler of HCS1.There is a beam crossing in the transverse planes x and y in the HCS2 section. Then, at the exit of the accelerating section the beam is really divergent with a maximum of 4.5mrad for a radius of 4.2mm. The first triplet and the following ones must obviously refocus the beam in the two planes.

With the actual Nov. 98 settings in the triplets, the evolution of the radius in PARMELA has completely different behaviour in each transverse plane. In the horizontal plane x, there is a cross-over between the two last triplets. In the vertical plane y, the maximum radius grows up to 15mm and is focused just by the last triplet with a large divergence of 8.1mrad. Thus the y cross-over occurs in the PETS. In addition, at the entrance of the 30 GHz sections, the maximum radius reaches 11.2mm and 9.1mm for x and y planes respectively. They are larger than the PETS aperture of 7mm radius and some particles must be lost at the PETS input.

According to these remarks, the use of Nov. 98 configuration in the inputs of PARMELA gives full transmission of the beam until the first PETS, but not after. The results in x and y directions are asymmetric and the diameter and divergence of the beam at the PETS entrance are too large. All theses points are not acceptable for the downstream line and may not correspond to the real trajectory and measurements with full transmissions in the shielded PETS at 10nC/bunch. In the next paragraph, slight variations on magnetic settings in PARMELA are proposed to obtain better transmission and a well adapted beam to the 30GHz PETS line.

Beam data for GUN4 with Virtual cathode.	**Magnetic element settings:**		
Photo-cathode diameter 11mm,	SNF100: 3100G	SNF110: 1170G	
10nC per bunch,	QFN130: 84.0G/cm	QFN131: -167.0G/cm	QFN132: 104.0G/cm
2998.55MHz repetition rate	QFN140: 54.0G/cm	QFN141: -53.0G/cm	QFN142: 54.0G/cm
	BHZE150: 5.6° 42.2MeV	BHZC151: -11.2° 42.2MeV	BHZE152: 5.6° 42.2MeV
HCS1: 3006.36MHz, 35.0MV/m, 1st bunch at -60.0° of rf crest	QFN160: 91.0G/cm	QFN161: -137G/cm	QFN162: 81G/cm
HCS2: 2990.74MHz, 35.0MV/m, 1st bunch at +25.0° of rf crest	QFN170: 92G/cm	QFN171: -163G/cm	QFN172: 82G/cm

	no bunch	Virtual cathode	in Sol1	in Sol2	in hcs1	out cp1 hcs1	in cp2 hcs1	out hcs1 / in hcs2	out cp1 hcs2	in cp2 hcs2	out hcs2 / in triplets	out triplets
z cm		0.0	10.2	37.8	65.0	75.9	135.4	159.8	182.4	242.2	253.1	1245.5
Trans.	**1**	100.0	100.0	100.0	100.0	100.0	100.0	100.0	100.0	100.0	100.0	100.0
%	**24**	100.0	100.0	100.0	100.0	100.0	100.0	100.0	100.0	100.0	100.0	99.9
	48	100.0	100.0	100.0	100.0	100.0	100.0	100.0	100.0	100.0	100.0	100.0
σ_z	**1**	.9893	.9879	.9933	1.0088	1.0155	.9706	.9529	.9394	.9393	.9393	.7867
mm	**24**	1.0179	1.0166	1.0244	1.0453	1.0520	1.0444	1.0444	1.0444	1.0444	1.0444	.8548
	48	1.0473	1.0462	1.0576	1.0861	1.0953	1.0907	1.0907	1.0907	1.0907	1.0907	.9246
γ	**1**	14.005	14.049	14.087	14.104	14.467	35.263	37.907	43.266	79.336	81.183	81.267
	24	13.105	13.148	13.181	13.195	15.157	42.193	44.764	49.112	84.282	86.606	86.729
	48	12.105	12.148	12.176	12.185	15.260	44.944	47.215	50.171	79.699	82.045	82.085
σ_γ/γ	**1**	1.3386	1.3822	1.7038	2.0590	1.7374	6.0562	5.8348	5.0666	1.5070	1.3181	1.3719
%	**24**	1.5145	1.5584	1.9018	2.2950	1.4447	3.0128	2.8706	2.8364	1.4614	1.3309	1.3668
	48	1.6962	1.7446	2.1226	2.5809	1.4967	.8564	.7963	1.1318	1.3932	1.3246	1.3936
$\frac{1}{2}(\sigma_x+\sigma_y)$	**1**	2.1637	3.5610	5.5275	6.7295	6.9494	2.8122	1.8406	1.1017	1.2947	1.5394	3.8997
mm	**24**	2.2422	3.7187	5.5289	6.4637	6.2579	2.4558	1.7402	1.1957	1.0614	1.2346	4.9653
	48	2.3214	3.9237	5.5303	6.1073	5.5473	1.7713	1.1512	.9136	1.6235	1.8321	3.0738
$\frac{1}{2}(\sigma_{x'}+\sigma_{y'})$	**1**	15.1135	14.2521	6.2402	4.2764	4.5488	3.9009	3.8759	3.7419	2.6861	2.6837	2.5594
mrad	**24**	15.9057	15.0644	5.5146	3.4235	2.3915	3.0654	3.0117	2.9448	2.2370	2.2192	2.3504
	48	17.1718	16.3773	4.5859	2.5201	1.9940	3.2632	3.1537	3.0340	2.3770	2.3425	2.0770
$\frac{1}{2}(\varepsilon_x+\varepsilon_y)$	**1**	48.11	57.94	60.35	62.11	126.29	73.65	71.20	70.26	69.26	69.38	87.68
mm.mrad	**24**	49.16	58.35	61.41	63.55	85.82	70.06	69.21	69.00	68.09	68.13	88.01
	48	51.22	59.99	64.11	66.38	70.12	69.70	69.65	69.44	69.21	69.18	79.14

Table 3: *Numerical values of the main beam characteristics along the Nov 98 layout simulated with 700 macro-particles. (ε_x and ε_y refer to the rms normalised emittances)*

III. Modified Nov. 98 settings for the 3GHz part of the drive beam

From the preceding case (Section II), several PARMELA simulations were done with small variations on the current of the first solenoid and the triplets. Each of the three simulated bunches of the train reacts differently in the transverse plane according to their different transverse sizes and energies. Moreover, the strong space charge for 10nC must be calculated with the 700 macro-particles of each run. For each modification, the three bunches and space charge must be simulated and the optimisation of the line is time consuming. Finally, the setting presented in table 1 is chosen as a good compromise between limited field variations from the experimental values, a beam well adapted to the PETS line and saved time.

The corresponding PARMELA results are reported in the figures 3, 4 and tables 4, 5. The beam dynamic is briefly commented in the following section. In the second section, the simulation and the effects of the magnetic bunch compressor are analysed.

III.1 PARMELA results for the modified Nov. 98 configuration

The magnetic field in the first solenoid is increased by 15% from 3100Gauss to 3500Gauss. The transverse beam is now more convergent at the input of the HCS1 section with a maximal radius below 10mm and a rms divergence divided by 2 from 4.2mrad to 2.1mrad. Then, the waist in x and y directions is displaced by 50cm towards the solenoids and located at the exit of HCS1 section. At the output of HCS2, the transverse beam dimensions are increased by 30% up to an rms radius of 1.7mm. But, the rms divergence is reduced from 2.6mrad to 1.6mrad and it is then less difficult to focuse the beam with the following first triplet.

The fields in the two extreme quadrupoles of the first triplet T1 are decreased by 10% from the experimental configuration, the settings of the second triplet T2 staying identical. The beam envelope is then more symmetrical between the two transverse planes. The over-increase of the y coordinate is avoided and the maxima are of 9mm in the two planes instead of 15mm in y direction and 9mm in x direction previously.

The variations of 5% to 15% introduced in the following triplets T3 and T4 give a convergent beam at the input of the 30GHz PETS line. At the entrance of the first PETS, the maximum radius varies only between 3mm and 4.5mm for a PETS section radius of 7mm. The rms divergence is below 1mrad with a dispersion of 0.5mrad. Moreover, the normalised rms transverse emittances ξ_x and ξ_y stay between the acceptable values of 70 to 75mm.mrad. As the figure 4 shows, the modified settings of the 3GHz line appear adapted to transmit all the beam without particles lost until the PETS. The corresponding results in the transverse plane will be used as input values for the study by A. Riche of the beam dynamics and transmission in the 30GHz line, wake-fields included.[5]

In the longitudinal plane (see table 4), the energy reaches 42.9±1.4MeV in the train with a rms dispersion in each bunch of about 1.6% or ±0.7MeV. The variations on the energy along the line are mainly induced by the settings of the two HCS sections.

On the phase delay, it is important to notice the following points. Due to the beam loading effects in the gun4, a phase delay of 6.3° between the first and last bunch is introduced at the beginning of the beam line. The magnetic bunch compressor adds different delays of flight time as a function of the bunch energy and deflection angle. In the present case, the phase dispersion in the train at the PETS entrance is of about 7° at 3 GHz or 70° at 30GHz for the last bunches. This value is high for the 30GHz section and a decrease of the power extraction may occur. Moreover, the bunch lengths at the PETS input are also lower or equal to 1mm rms. But this result obtained with the nominal phasing -60° and 25°of the HCS may be optimised in the simulations (and are effectively modified in the experiments), in order to both increase the longitudinal bunch compression and reduce the phase shift in the train.

The bunch compressor is studied in more details in the next section.

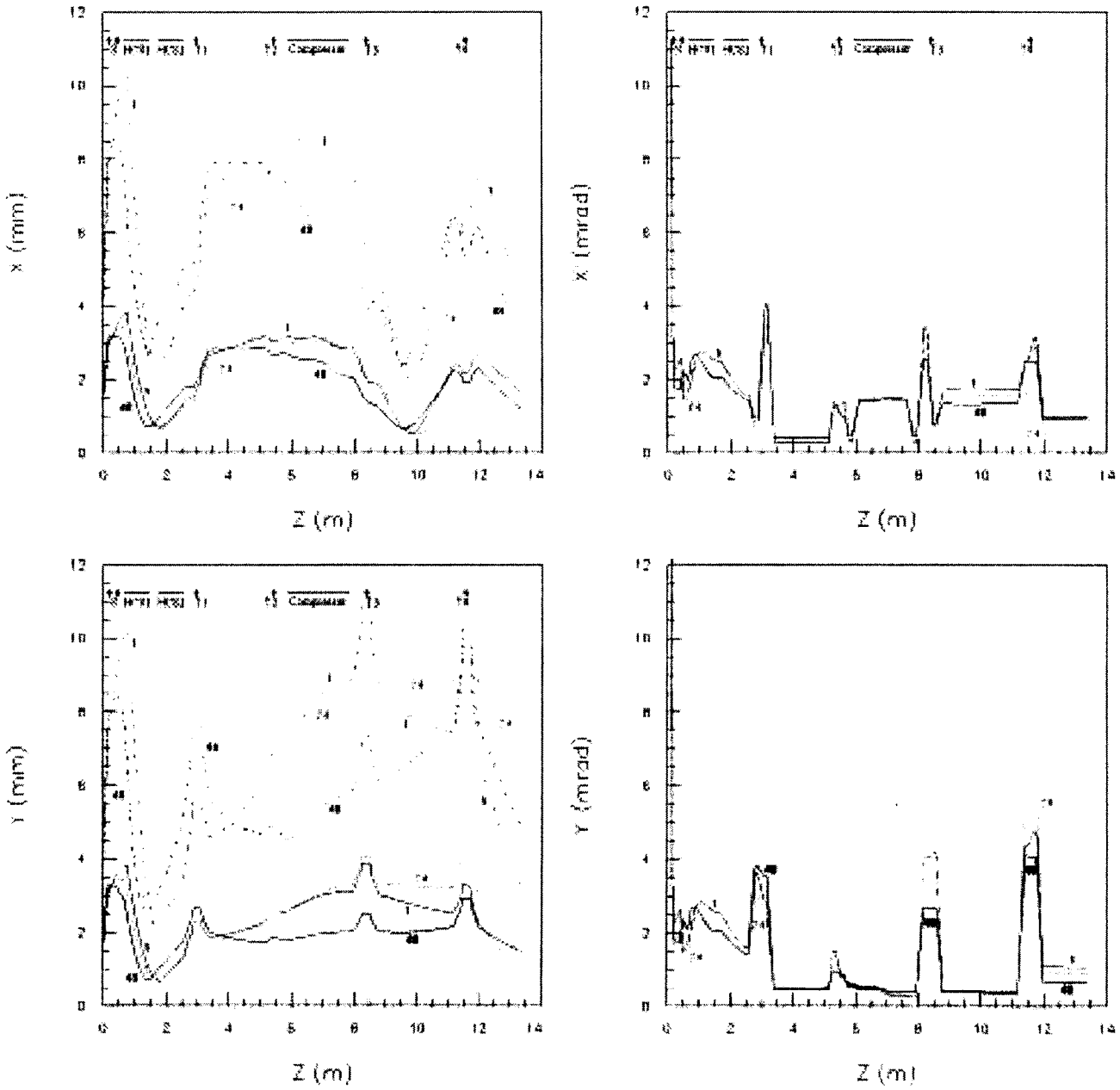

Figure 3: *x, y, x' and y' variations along z axis for the modified Nov 98 configuration simulated with 700 macro-particles. The numbers 1, 24 and 48 (and the red, green and blue colours) refer to the 1st, 24th and 48th bunches respectively. Rms values are drawn by solid lines, maxima by dashed lines.*
(Note the change of scales compared with figure 2.)

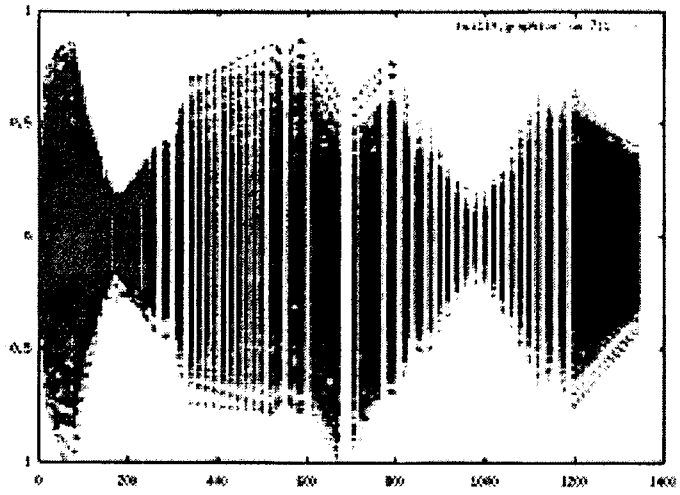

(a) 1st bunch, X (cm) in function of Z (cm)

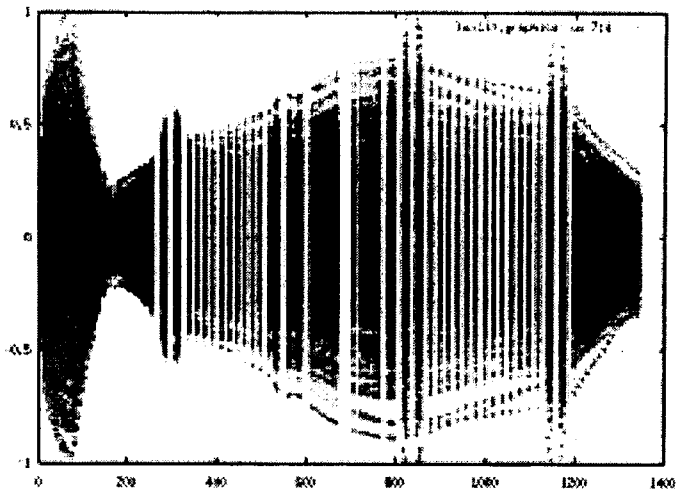

(b) 1st bunch, Y (cm) in function of Z (cm)

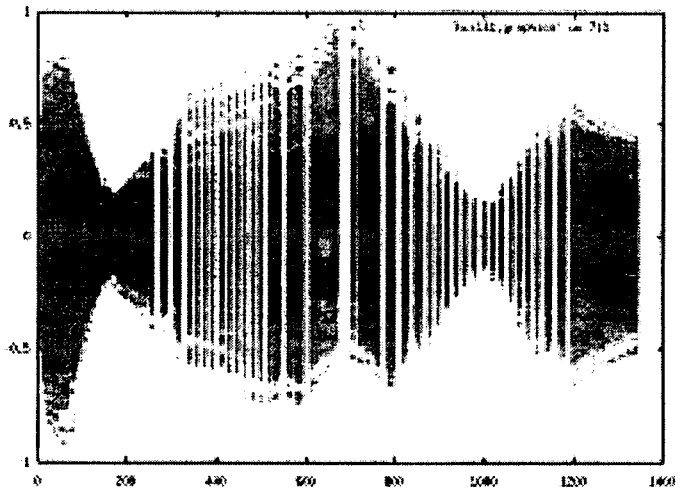

(c) 24th bunch, X (cm) in function of Z (cm)

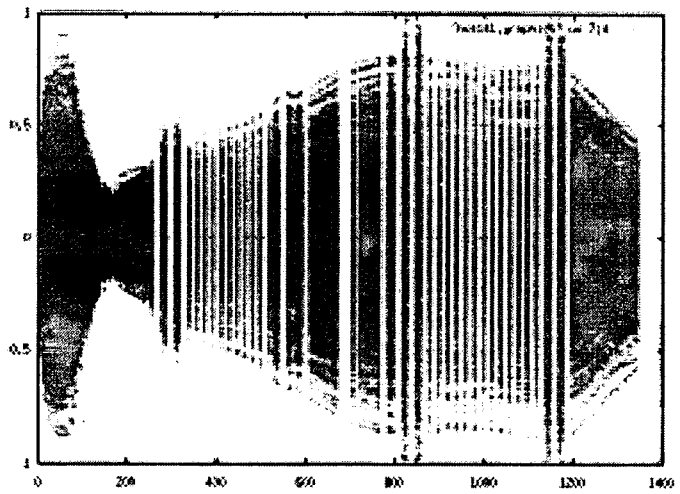

(d) 24th bunch, Y (cm) in function of Z (cm)

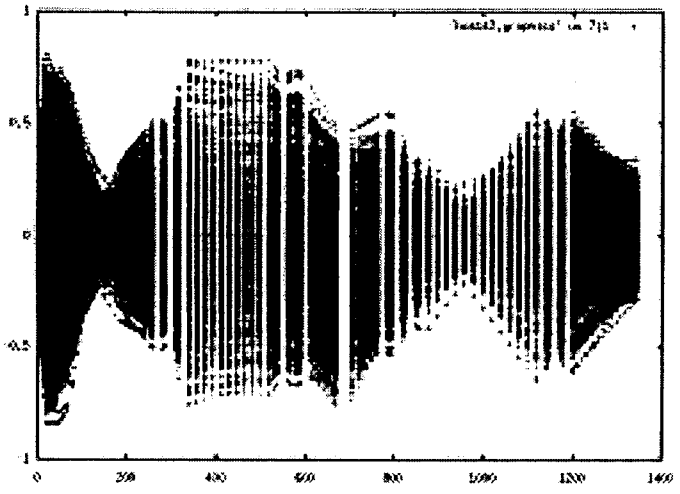

(e) 48th bunch, X (cm) in function of Z (cm)

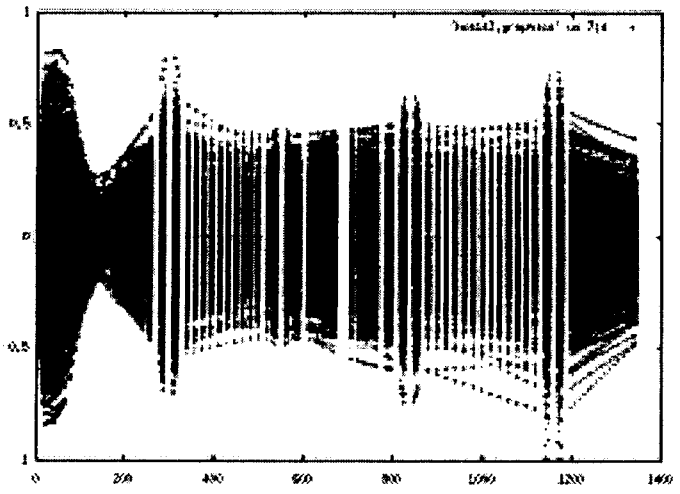

(f) 48th bunch, Y (cm) in function of Z (cm)

Figure 4: *x and y coordinates of the 700 simulated macro-particles in function of z axis for the modified Nov 98 configuration.*

PARMELA SIMULATIONS: HCS140, HCS141, HCS142

HCS1 and HCS2: The 13 cavities between the couplers are considered as travelling wave cells with 11pi/12 phase shift. The couplers are represented by fully standing wave cells and the field levels are *1.5 and *0.88 for respectively input and output couplers.

HCS1:	1st bunch,	34.8MV/m,	-60.0° of rf crest
at 3006.36MHz	24th bunch,	29.2MV/m,	-37.5° of rf crest
	48th bunch,	26.4MV/m,	-15.0° of rf crest
HCS2:	1st bunch,	34.9MV/m,	+25.0° of rf crest
at 2990.74MHz	24th bunch,	30.4MV/m,	+2.5° of rf crest
	48th bunch,	26.3MV/m,	-20.0° of rf crest

Beam data for *Gun4* and *Virtual cathode*.
Photo-cathode diameter 11mm, 10nC per bunch,
2998.55MHz repetition rate

Magnetic element settings:
Sol1: 3580G
Sol2: 1170G
T1: 77.0G/cm, -167.0G/cm, 95.5G/cm
T2: 54.0G/cm, -53.0G/cm, 54.0G/cm
BZ: 5.6°, 11.2°, 5.6° at 42.2MeV
T3: 76.6G/cm, -129.0G/cm, 76.6G/cm
T4: 106.0G/cm, -167.0G/cm, 94.5G/cm

		Bunch	*Vir. Cat.*	*In Sol1*	*In Sol2*	*In HCS1*	*In HCS2*	*In T1*	*In T2*	*In Bz*	*In T3*	*In T4*	*PETS1*
Z el.	cm		0.0	10.2	37.8	65.1	159.8	253.1	515.9	588.7	795.5	1117.0	1340.5
σ_z	mm	1st	0.989	0.988	0.993	1.011	0.961	0.948	0.948	0.948	0.881	0.879	0.879
		24th	1.018	1.017	1.024	1.048	1.050	1.050	1.050	1.050	0.986	0.984	0.983
		48th	1.047	1.046	1.058	1.091	1.099	1.099	1.099	1.099	1.032	1.030	1.030
$\langle\gamma\rangle$		1st	14.03	14.05	14.07	14.08	37.79	81.14	81.22	81.22	81.22	81.21	81.14
		24th	13.03	13.15	13.17	13.17	44.68	86.61	86.67	86.68	86.69	86.67	86.64
		48th	12.13	12.15	12.16	12.16	47.19	82.05	82.08	82.08	82.07	82.08	82.03
σ_γ/γ	%	1st	1.34	1.38	1.75	2.17	5.86	1.31	1.38	1.40	1.40	1.49	1.57
		24th	1.51	1.55	1.95	2.44	2.91	1.36	1.42	1.43	1.44	1.51	1.57
		48th	1.69	1.74	2.19	2.79	0.92	1.28	1.33	1.35	1.36	1.46	1.59
$\Delta\varphi$	deg.	1st	0.0	0.0	0.0	0.0	0.0	0.0	0.0	0.0	0.0	0.0	0.0
		24th	2.8	2.9	3.3	3.7	2.9	2.7	2.7	2.7	-0.5	-0.4	-0.5
		48th	6.3	6.6	7.5	8.4	7.6	7.4	7.3	7.4	6.9	7.0	6.9

Table 4: *Numerical values of the main longitudinal beam characteristics along z axis for the modified Nov. 98 configuration. The phase delay $\Delta\varphi$ includes the shift du to the beam loading of the gun4*

		Bunch	*Vir. Cat.*	*In Sol1*	*In Sol2*	*In HCS1*	*In HCS2*	*In T1*	*In T2*	*In Bz*	*In T3*	*In T4*	*PETS1*
Z el.	cm		0.0	10.2	37.8	65.1	159.8	253.1	515.9	588.7	795.5	1117.0	1340.5
σ_x	mm	1st	1.47	2.40	3.34	3.77	0.79	1.33	3.19	3.20	2.84	2.43	1.59
		24th	1.52	2.51	3.27	3.45	0.74	1.25	2.94	3.00	2.85	1.89	1.91
		48th	1.57	2.65	3.17	3.02	0.77	1.71	2.87	2.70	2.04	2.26	1.14
σ_y	mm	1st	1.58	2.62	3.51	3.82	0.78	1.37	2.28	2.57	3.14	2.52	0.99
		24th	1.64	2.74	3.41	3.45	0.75	1.29	2.26	2.60	3.32	3.23	1.90
		48th	1.70	2.89	3.26	2.97	0.80	1.74	1.72	1.78	2.04	2.17	1.47
$\sigma_{\gamma\beta_x}$	$.10^{-3}$	1st	131.9	134.5	35.7	24.4	92.8	127.8	31.0	27.1	27.6	136.7	72.4
		24th	130.4	133.1	25.3	18.8	88.7	117.3	34.7	23.7	24.4	132.1	43.4
		48th	131.7	134.6	20.8	23.6	96.6	116.8	24.0	41.4	41.1	106.8	79.9
$\sigma_{\gamma\beta_y}$	$.10^{-3}$	1st	144.7	147.4	36.3	24.1	95.5	131.0	40.4	50.1	22.0	27.8	85.7
		24th	142.9	145.8	25.4	19.4	90.2	118.6	46.0	56.7	25.0	22.0	77.6
		48th	143.3	146.3	20.7	24.8	96.9	116.8	40.5	42.2	34.9	36.8	54.5
$\sigma_{x'}$	mrad	1st	9.42	9.60	2.54	1.74	2.46	1.57	0.38	0.33	0.34	1.68	0.89
		24th	9.96	10.15	1.92	1.43	1.99	1.35	0.40	0.27	0.28	1.52	0.50
		48th	10.89	11.12	1.72	1.95	2.05	1.42	0.29	0.50	0.50	1.90	0.97
$\sigma_{y'}$	mrad	1st	10.34	10.52	2.59	1.72	2.53	1.61	0.50	0.62	0.27	0.34	1.06
		24th	10.92	11.12	1.93	1.48	2.02	1.37	0.53	0.65	0.29	0.25	0.90
		48th	11.86	12.09	1.71	2.04	2.05	1.42	0.49	0.51	0.42	0.45	0.66
ξ_x	mm.mrad	1st	49.0	57.3	59.5	61.2	63.9	63.4	64.6	65.3	69.1	70.7	72.8
		24th	50.1	58.3	60.3	61.9	63.6	63.3	63.8	64.5	67.0	68.2	69.0
		48th	52.2	62.8	65.9	67.3	67.5	67.4	68.7	69.3	71.6	72.4	73.8
ξ_y	mm.mrad	1st	47.4	59.2	62.5	63.2	65.7	65.3	66.5	66.5	66.4	67.0	69.7
		24th	48.5	59.6	64.3	65.2	66.4	66.1	67.2	67.2	68.0	68.8	75.1
		48th	50.5	61.6	67.7	68.7	68.8	68.8	69.6	69.6	69.4	68.8	69.1

Table 5: *Numerical values of the main transverse beam characteristics along z axis for the modified Nov. 98 configuration. (ε_x and ε_y refer to the rms normalised emittance)*

III.2 On magnetic bunch compressor simulation

The influence of the magnetic bunch compressor is really important on the longitudinal beam dynamics before the PETS sections. So, variations of bunch compression and phase delay in the train are studied in this paragraph. In particular, variations with magnet current are shown. Both, the results of MATHCAD analytical calculations and PARMELA simulations are used, the phenomena are related to the CTF2 drive beam configuration.

For all the results presented in figures 5 to 8, the train before the magnetic compressor is the one obtained from the PARMELA simulations in the modified Nov. 98 configuration. So, 700 macro-particles are considered. The bunch energies are of 41.5±0.58, 44.3±0.63 and 41.9±0.56 MeV for the 1st , 24th and 48th bunches respectively (average value ± rms). In phase, the rms lengths are of ±3.4°, ±3.8° and ±3.9° for the three bunches.

The figure 5 shows the bunch compression as a function of the magnet current for PARMELA and MATHCAD calculations. In MATHAD model, the space charge effects are neglected because the energies are higher than 41MeV. First, it appears that the variations have similar shapes for the two models and differences stay below 8%. Secondly, the maximum bunch compression of about 70% is reached for a deflection angle of about 10-11°. For the nominal Nov 98 setting with 5.6°, the compression is only of 88% which corresponds to $\Delta\varphi/\Delta E$ equal to 0.73°/MeV or 0.67ps/MeV. If the intra- bunch energy spread was increased before the compressor thanks to optimisation of the HCS phases, the bunch length could be more reduced than for this nominal configuration.

If the longitudinal emittance of the bunch is reduced by suppressing 10% of the macro-particles as on the figure 9, the energy spread is reduced by about 10% but the bunch lengths stay nearly the same with a phase-sigma 1% smaller. Then, the maximum compression is reached for higher magnet field (see figure 6) but with an actually better compression of 55%. At the nominal angle 5.6°, the compression is of 83% and $\Delta\varphi/\Delta E$ is 0.96°/MeV or 0.89ps/MeV. So, if experimentally bunches have no aberrant particle and better correlation behind the compressor, it allows to obtain significant increase of the bunch compression.

An other phenomena occurs in the bunch compressor: the phase delay between the bunches as a function of their average energies (see figure 7). The extreme bunches 1 and 48 have lower energy, their trajectories become longer and they arrive later than the mid bunch 24. This corresponds to 0.96°/MeV for a deflection of 5.6° and increases non-linearly with the bunch current to 4.6°/MeV for 11° deflection angle.

In the CTF2 line, the beam loading for 48×10nC bunches in the gun 4 induces a phase shift at its exit of about 6.3° between the first and last bunch. This shift is complemented by a linear decrease of the energy at the gun exit. Then, in the drift tubes and the HCS sections, the phase shift continues to rise as a function of the relative gain of energy. The maximal delay is of 7.4° for the 48th bunch at the entrance of the spectrometer magnet. The compressor adds its own flight delay, so that the phase delay of the first bunches is decreased but the delay of the last bunches is increased because of the varying bunch energy. Finally, the last bunches arrive with a delay of 7° at 3GHz. In the PETS sections, the phase delay amounts to 70° at 30GHz and reduces the efficiency of the 30GHz power extraction to cos70°=34%. For this reason, the deflection angle in the bunch compressor is experimentally restricted to about 7°.

In the figure 8, the transverse emittance simulated with PARMELA is shown as a function of the magnet current. An upper limit also appears for about 7° if a reasonable horizontal emittance smaller than 80mm.mrad is maintained. On the other hand, the emittance stays stable in the vertical plane.

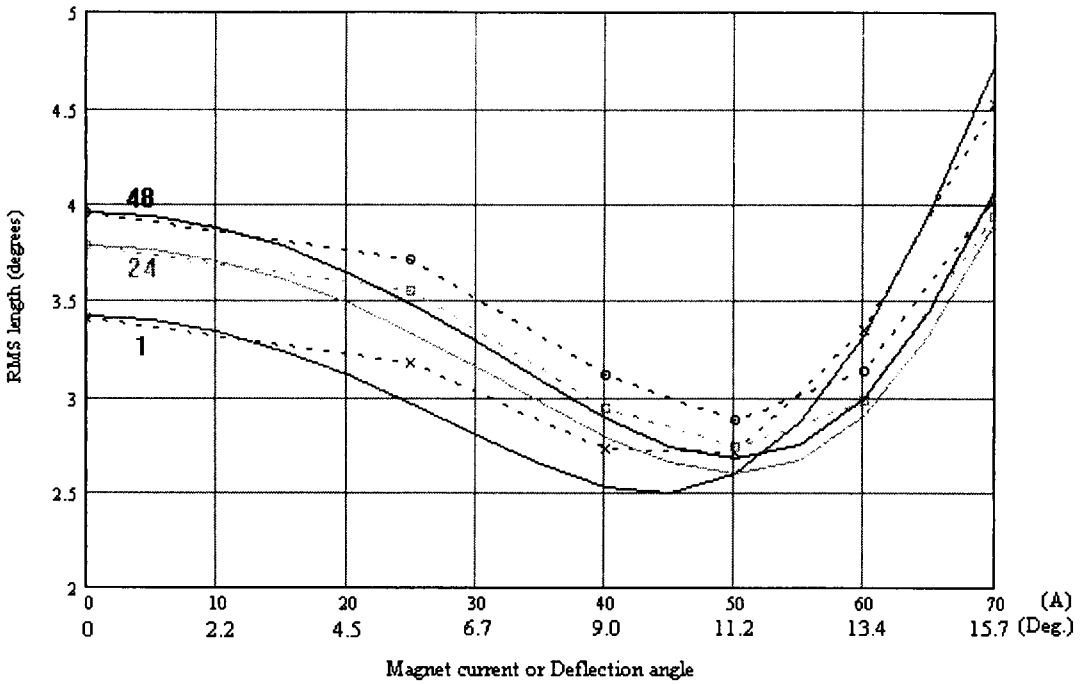

Figure 5: *Variations of the rms length of the three bunches 1, 24 and 48 as functions of the bunch compressor strength for 700 particles in each bunch. The solid line mark MATHCAD calculation, the dashed line PARMELA simulation.*

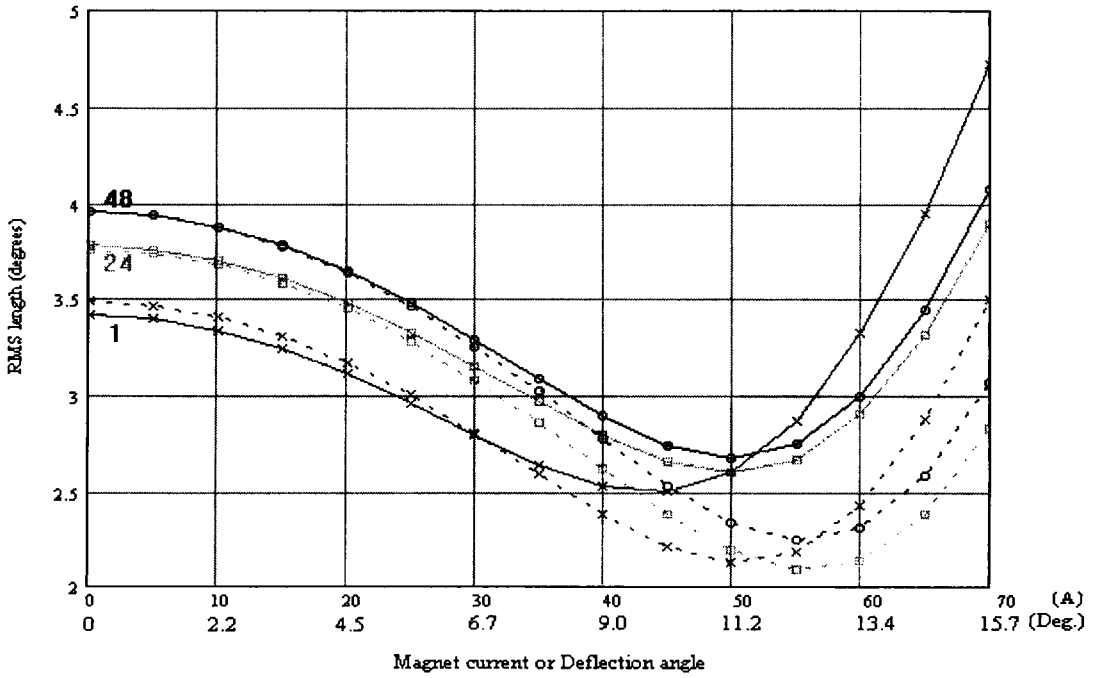

Figure 6: *Variations of the rms length of the three bunches 1, 24 and 48 as functions of the bunch compressor strength. Comparaison between 100% of bunch particles in solid line and only 90% in dashed line*

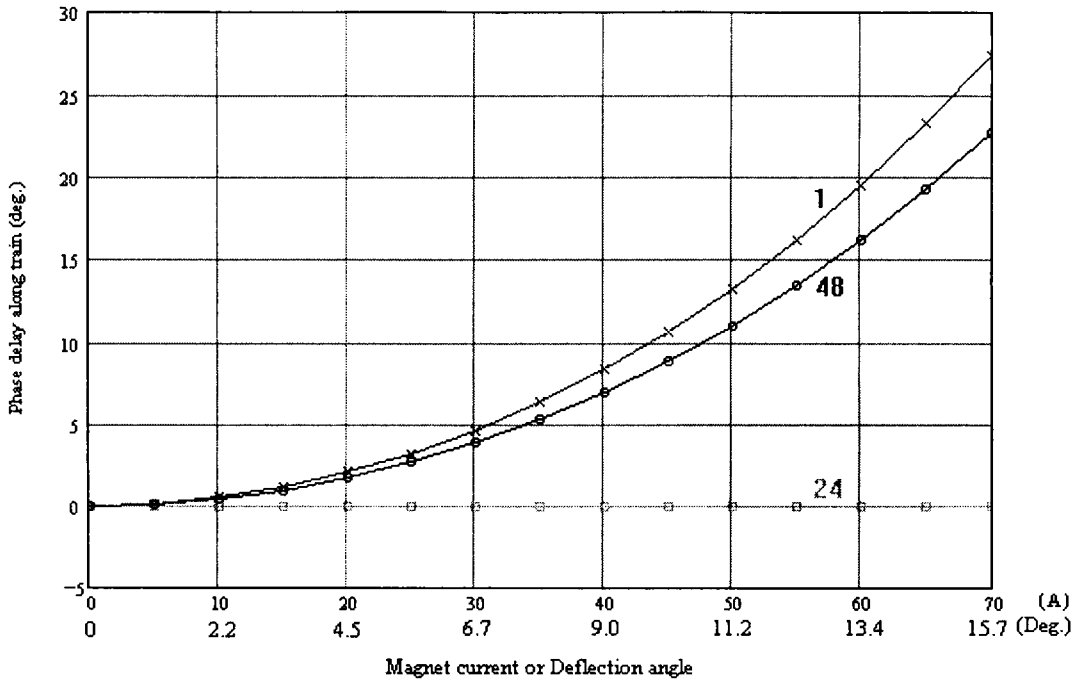

Figure 7: *Variations of the phase delay of the three bunches 1, 24 and 48 as functions of the bunch compressor*

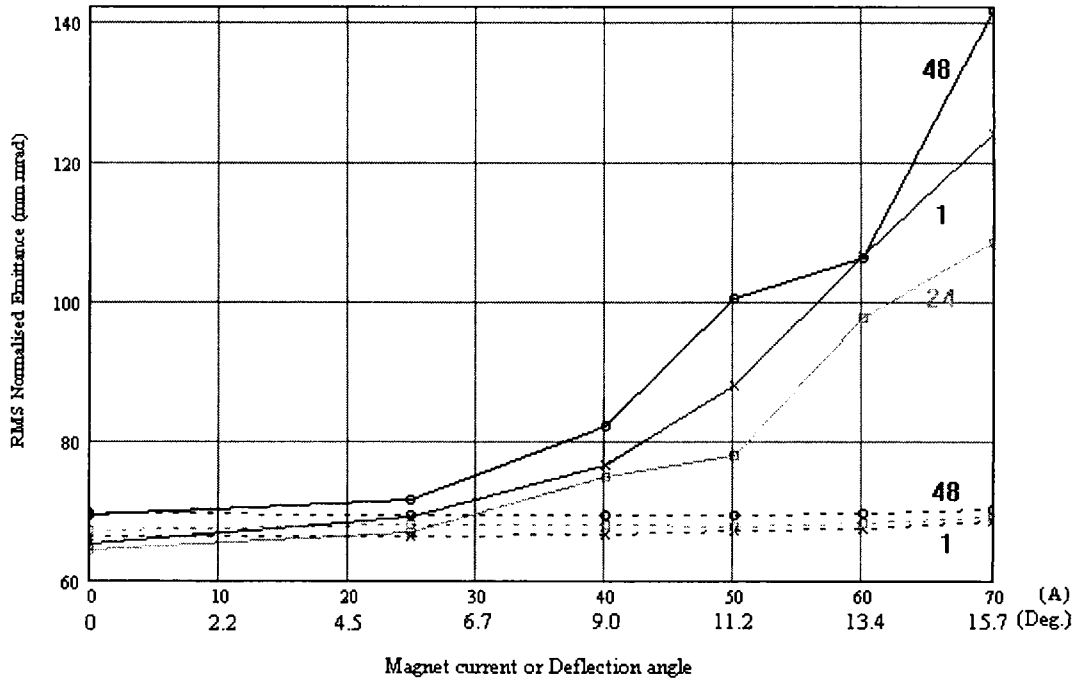

Figure 8: *PARMELA variations of the normalised rms emittances ε_x and ε_y of the three bunches 1, 24 and 48 as functions of the bunch compressor strength. The solid and dashed lines show the emittances in the x and y plane respectively.*

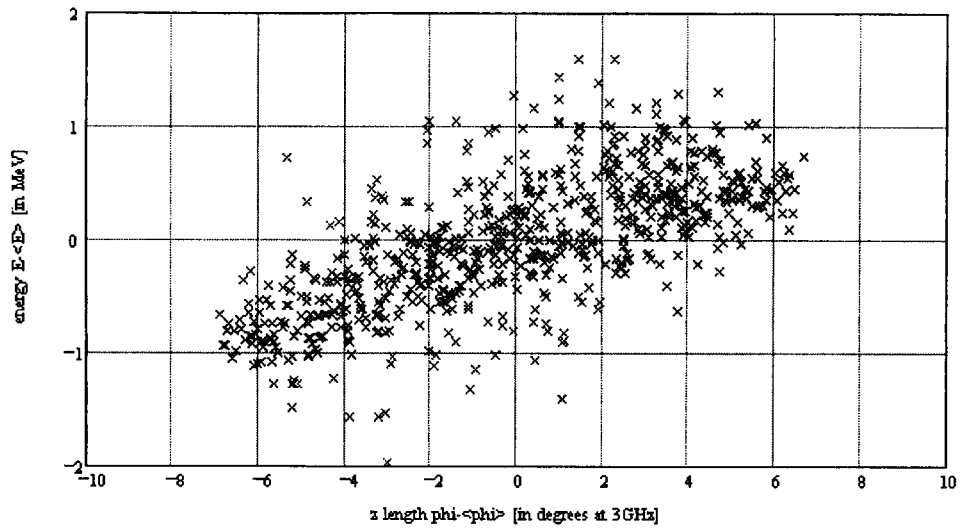

(a) First bunch

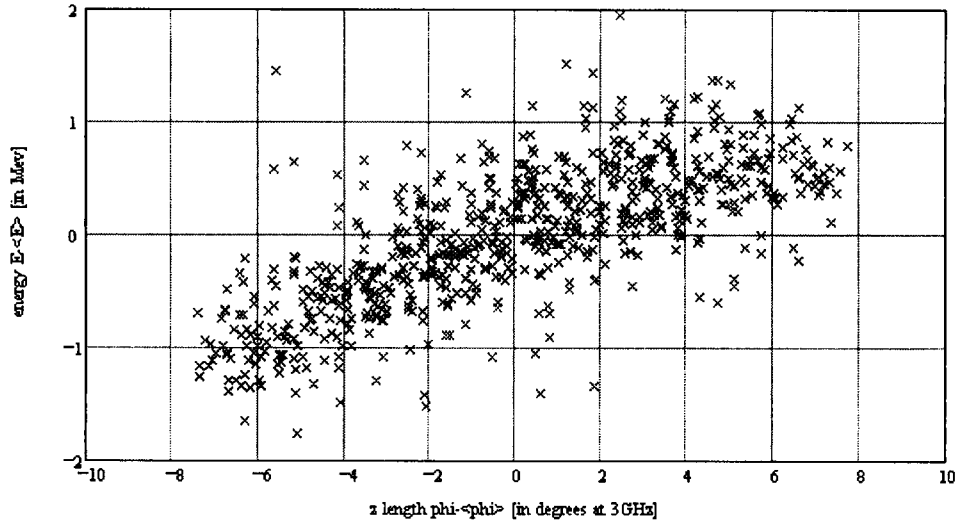

(b) 24th bunch

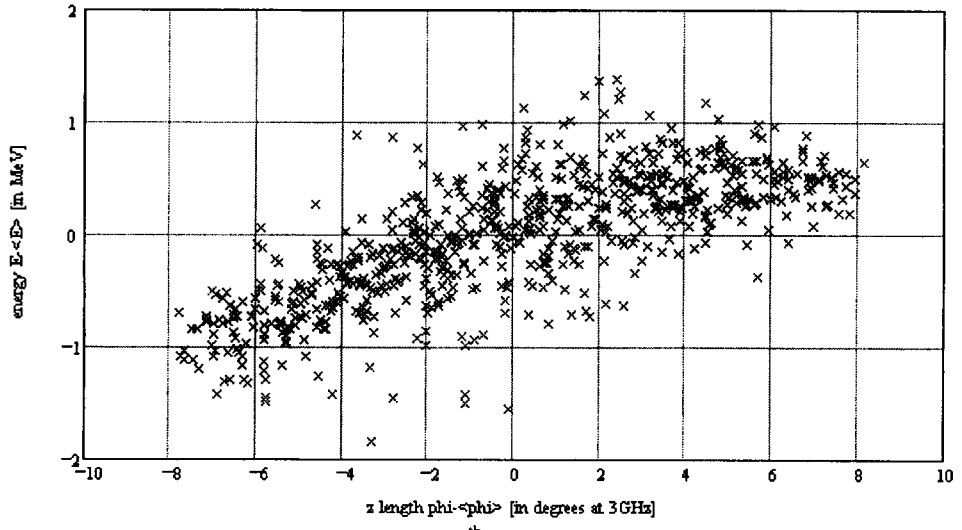

(c) 48th bunch

Figure 9: *Longitudinal space scattering plot of the 700 particles in the tree bunches 1, 24 and 48. The aberrant particles of the halo ("red points") are suppressed to obtain only the 90% of particles.*

III.3 Effect of a deflection variation in HCS in the downstream line

In the previous sections, simulations with the modified Nov 98 settings show that transmission and adaptation of the beam are realised at the PETS entrance. But, PARMELA simulations neglect the wake fields in HCS. In PARMELA simulations, it is possible to stop the space charge in the HCS and to analyse the effects of the variation of the HCS deflection on the beam in the downstream line. Then, it is possible to compare this deflection with the one induced by the wake fields calculated separately.

Special PARMELA simulations have been made with space charge effects included from the cathode to the entrance of HCS and without space charge from HCS to the end of the line. The inputs of the modified Nov 98 configuration are used. For the three bunches 1, 24 and 48, the vertical and horizontal trajectories of the 700 macro-particles are traced along the beam axis on the figure 10.

Not very important modifications in the transverse plane are induced when the space charge is switched off (compare to fig. 4). In HCS1 and 2, the horizontal waist between the triplet 3 and 4 is shifted by about 0.15m towards the PETS. At the entrance of the PETS, the beam diameter is reduced by 0.5 to 2mm depending of the bunches energy.

An approximated calculation of the radial space charge forces in HCS1 was performed by R. Bossart [6] in the case of the last bunch. It was found that the beam divergence due to the space charge is about 0.5mrad in our case.

For comparison, the deflection induced by the transverse wake field in HCS1 has also been calculated by R. Bossart [7]. Here, a brief remark is given. Only the first dipole mode of HCS1 at 4120MHz is assumed. The phase advance per bunch is $2\pi*4120/2991=1.37*2\pi$.After three bunches the deflection voltage vector is nearly null. The maximum deflection is given to bunches 2 and 3, 5 and 6 etc and is of the order of 0.28mrad for 1mm offset. This periodicity of 3 bunches on the wake deflection significantly reduces the transverse effects. Otherwise, the periodicity 3 in the bunch displacement in the train may be the experimental signature of the presence of wake field in HCS.

As the predicted wake field deflection of 0.28mrad is actually lower than the space charge deflection of 0.5mrad, we can expect that the effects of HCS wakes on the downstream line will be lower than those induced by space charge forces. The transmission and adaptation to PETS should then be possible by a slight optimisation of the triplets and a correction of the beam size at the PETS entrance.

For verification and more precisions, the reader should refer to the wake field simulations in the HCS structure performed by A. Riche and presented in [5].

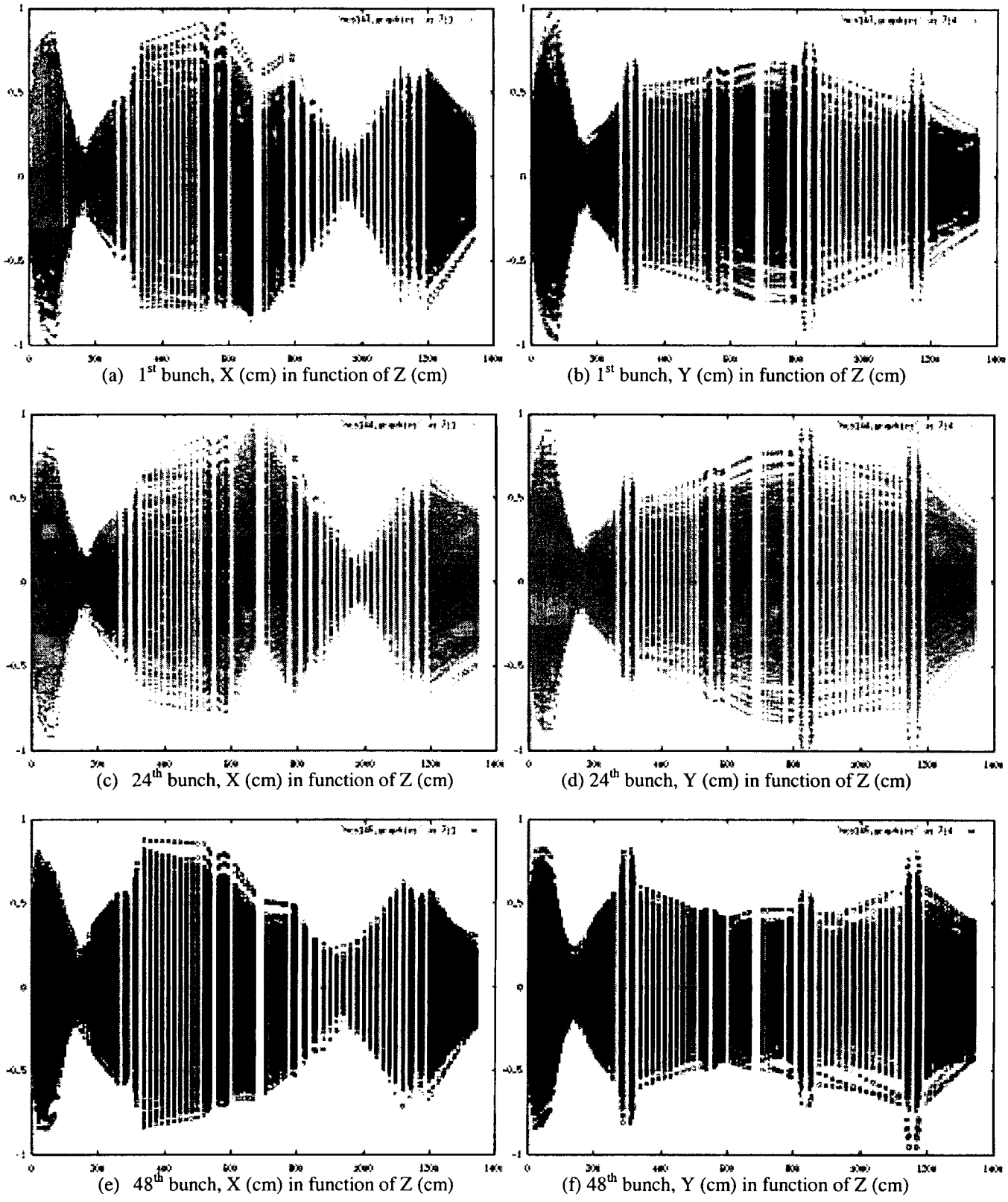

(a) 1st bunch, X (cm) in function of Z (cm)

(b) 1st bunch, Y (cm) in function of Z (cm)

(c) 24th bunch, X (cm) in function of Z (cm)

(d) 24th bunch, Y (cm) in function of Z (cm)

(e) 48th bunch, X (cm) in function of Z (cm)

(f) 48th bunch, Y (cm) in function of Z (cm)

Figure 10: *x and y envelopes in function of the z axis for the modified Nov 98 configuration simulated with 700 macro-particles. The space charge is not included from the HCS1 structure to the end of the line but considered before.*

Conclusion:

PARMELA particle-tracking program has allowed to successfully simulate the CTF2 drive beam along the 3GHz part of the line. From the actual Nov 98 settings, the triplet currents had to be slightly modified by 5% to 15%. Then, the simulated beam transmission is well matched up to the entrance of the 30GHz PETS section. The beam is focused with a waist common to all bunches and energies in the PETS. At the entrance of the first PETS, the beam size reaches no more than 4.5mm radius with a divergence below 1mrad. All particles of the 10nC bunches are transmitted to the PETS and the obtained transverse beam characteristics have been used for wake-field studies in the PETS line carried by A. Riche [5].

Secondly, the simulated 10nC bunches generated by the laser spot of 5.5mm radius present a transverse size up to 13mm radius at the entrance of HCS1. It shows that an enhancement in the laser spot size and bunch charge may be dangerous and induce particle losses at the HCS1 input. Moreover, because of the strong focusing and the existence of a waist in the accelerating HCS sections, the settings of the first triplet must be carefully tuned in order to rematch the beam.

In the previous sections, according to the test with space charge suppressed, it is verified that the space charge in the HCS sections do not disturb dangerously the beam in the compressor and the downstream line. It can therefore be expected that the HCS wake-field effects will be of the same order or lower than the latter and not generate a source of difficulties.

Finally, the model of the bunch compressor was verified. Some particularities of its behaviour were pointed out. The magnitude but also the quality of the bunch correlation at the entrance of the compressor determine the efficiency of the compression together with the magnet current. And the deflection angle must be limited to 7° in order to keep the phase shift in the train and the emittance growth acceptable for the beam in the 30Ghz line downstream.

Acknowledgements:

Many thanks to the CTF team and especially to the group involved in regular discussions and meetings. Then, I want name and express my gratitude to R. Bossart, H. Braun, G. Guignard, A. Riche, and M. Valentini for their work, advice and interest.

References:

[1] "The CLIC test facility: CTF2 a two-beam test accelerator for linear collider Studies", CTF2 design report, CLIC Team, CERN/PS/96-14 (LP), June 96

[2] "The PARMELA program", B. Mouton, LAL/SERA 93-455, Sept. 93

[3] "MAFIA simulations on gun 4", M. Dehler, Private Communication, 97

[4] "Beam dynamics in the accelerating RF structures of the CTF2 drive beam simulated with PARMELA particle tracking program", M. Chanudet, CLIC Note 409, July 99

[5] "Wake-fields in the HCS accelerator and CTS power line of the CLIC test facility (CTF2) – Simulation with program WAKE", A. Riche, CLIC Note 430, April 2000

[6] "Radial space charge forces in CTF2", R. Bossart, Private communication, June 99

[7] "Asynchronous excitation of the HCS1 wake-field", R. Bossart, Private communication, June 99

[8] "Summary of the CTF2 beam dynamics work group", G. Guignard, M. Chanudet-Cayla, A. Riche, CERN CTF Note 00-04, Feb. 2000

[9] "Intensity limitations of the drive beam accelerator CTF2", R. Bossart, CERN PS/RF/Note 2000-007